The Journal of Experimental Medicine

Aquaporin-4–binding autoantibodies in patients with neuromyelitis optica impair glutamate transport by down-regulating EAAT2

Shannon R. Hinson,[1] Shanu F. Roemer,[2] Claudia F. Lucchinetti,[2] James P. Fryer,[1] Thomas J. Kryzer,[1] Jayne L. Chamberlain,[3] Charles L. Howe,[2,3] Sean J. Pittock,[1,2] and Vanda A. Lennon[1,2,3]

Departments of [1]Laboratory Medicine and Pathology, [2]Neurology, and [3]Immunology, Mayo Clinic College of Medicine, Rochester, MN 55905

Neuromyelitis optica (NMO)–immunoglobulin G (IgG) is a clinically validated serum biomarker that distinguishes relapsing central nervous system (CNS) inflammatory demyelinating disorders related to NMO from multiple sclerosis. This autoantibody targets astrocytic aquaporin-4 (AQP4) water channels. Clinical, radiological, and immunopathological data suggest that NMO–IgG might be pathogenic. Characteristic CNS lesions exhibit selective depletion of AQP4, with and without associated myelin loss; focal vasculocentric deposits of IgG, IgM, and complement; prominent edema; and inflammation. The effect of NMO–IgG on astrocytes has not been studied. In this study, we demonstrate that exposure to NMO patient serum and active complement compromises the membrane integrity of CNS–derived astrocytes. Without complement, astrocytic membranes remain intact, but AQP4 is endocytosed with concomitant loss of Na^+-dependent glutamate transport and loss of the excitatory amino acid transporter 2 (EAAT2) . Our data suggest that EAAT2 and AQP4 exist in astrocytic membranes as a macromolecular complex. Transport-competent EAAT2 protein is up-regulated in differentiating astrocyte progenitors and in nonneural cells expressing AQP4 transgenically. Marked reduction of EAAT2 in AQP4-deficient regions of NMO patient spinal cord lesions supports our immunocytochemical and immunoprecipitation data. Thus, binding of NMO–IgG to astrocytic AQP4 initiates several potentially neuropathogenic mechanisms: complement activation, AQP4 and EAAT2 down-regulation, and disruption of glutamate homeostasis.

CORRESPONDENCE
Vanda A. Lennon:
lennon.vanda@mayo.edu

Neuromyelitis optica (NMO) is currently the best-defined acquired inflammatory demyelinating disorder of the central nervous system (CNS) (1, 2). NMO attacks optic nerves and spinal cord selectively and repeatedly. The preferential distribution and severity of lesions in NMO is poorly understood. Clinical, histopathological, and immunobiological observations support a pathogenic role for an IgG autoantibody specific for the astrocytic water channel aquaporin-4 (AQP4), and the severity of acute NMO is ameliorated by antibody-depleting therapies (1). In contrast to most inflammatory CNS demyelinating disorders, tissue destruction in NMO is profound. In addition to white matter lesions, NMO characteristically exhibits central necrosis of spinal

cord gray matter (3). Histopathological CNS lesions lack AQP4 (4) and show deposition of IgM and IgG and products of complement activation in a vasculocentric pattern that coincides with the normal distribution of AQP4 (4, 5). Until recently, NMO was considered a rare and severe variant of multiple sclerosis (MS). However, the advent of serological testing for AQP4-IgG has revealed that NMO and its inaugural forms are more common than previously recognized. They tend to be misdiagnosed as MS, which lacks a specific biomarker (1).

We recently demonstrated in vitro the pathogenicity of NMO-IgG for nonneural cells transgenically expressing AQP4, and that NMO serum IgM is not AQP4 specific. Binding of NMO-IgG to the extracellular domain of AQP4 reversibly down–regulates its plasma membrane expression (6). In the presence of active complement, binding of NMO-IgG to surface AQP4 initiated robust complement activation and rapid loss of the target cell membrane's integrity. We concluded that the abundant IgM deposits in CNS lesions of NMO patients are plasma-derived and enter through the breached blood–brain barrier after initial focal activation of complement by AQP4-IgG (6). Multisystem autoimmune diseases frequently accompany NMO (7), and the elevated circulating IgM that is characteristic of multisystem autoimmunity has rheumatoid factor–like properties that could amplify the CNS inflammatory response in NMO (6).

A recent report that astrocytes lacking AQP4 express a reduced level of the astrocytic Na^+-dependent excitatory amino acid transporter 2 (EAAT2; homologue of rodent GLT-1 [8]) led us to hypothesize that if NMO-IgG altered the expression of EAAT2 in astrocyte membranes, this might impair glutamate homeostasis (6). Resulting overstimulation of glutamate receptors in neurons and oligodendrocytes could contribute indirectly to the pathobiology of NMO. EAAT2 accounts for >90% of glutamate uptake in the CNS (9), is critical for clearing glutamate from excitatory synapses, and is expressed selectively in astrocytes.

In this study, we demonstrate that: (a) when active complement is present, binding of NMO-IgG to AQP4 in astrocyte membranes causes membrane lesioning; (b) in the absence of complement, NMO-IgG causes antigen-specific removal of AQP4 from astrocytic membranes with reduction of Na^+-dependent glutamate transport and loss of surface EAAT2; (c) transgenic expression of AQP4 in nonastrocytic cells, and physiological up-regulation of AQP4 in differentiating astrocytes, induces surface EAAT2 expression; (d) AQP4 and EAAT2 exist in astrocytic membranes as a macromolecular complex; and (e) regions of AQP4 loss in NMO spinal cord lesions are deficient in EAAT2.

RESULTS AND DISCUSSION
NMO–IgG binding to primary astrocytes induces AQP4 modulation and complement activation

We monitored AQP4 distribution after applying NMO or control serum to cerebral astrocytes. Serum containing NMO-IgG, but not control serum, induced rapid down-regulation of surface AQP4 (Fig. 1 A). AQP4 coalesced in cytoplasmic vesicles reminiscent of those observed in GFP-AQP4–transfected nonneural cells exposed to NMO-IgG (6).

We evaluated the complement-activating capacity of NMO-IgG binding to astrocytic AQP4 by including complement with NMO or control serum, and processing the cells for flow cytometric analysis of propidium iodide influx. In the presence of NMO-IgG and active complement, plasma membrane permeability increased by approximately twofold (P < 0.007; Fig. 1 B). With heat-inactivated complement, we observed no discernible effect with control serum or NMO serum (Fig. 1 B). Activation of early complement components by IgG binding to the extracellular domain of AQP4
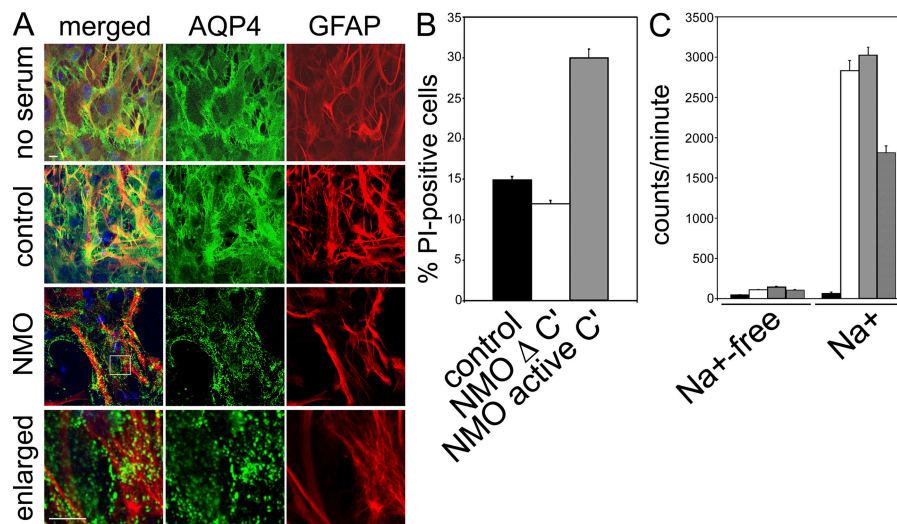
Figure 1.   In primary astrocytes, NMO–IgG induces internalization of AQP4, impairment of glutamate uptake, or complement activation. (A) Plasma membrane AQP4 (green) and cytoplasmic GFAP (red) after exposure to no human serum, control patient serum, or NMO patient serum. Serum containing NMO-IgG causes rapid translocation of surface AQP4 into cytoplasmic vesicles. Boxed area is enlarged in bottom images. Bars, 10 μm. (B) Quantitation of membrane permeability after exposure to control or NMO serum. Increase in permeability to propidium iodide (PI) greater than twofold by NMO serum required active complement (Δ C' = inactivated complement). (C) Uptake of L-[³H]glutamate (±Na⁺-containing buffer) without human serum (white column) or in control (gray column) or NMO serum (crosshatched column). Excess unlabeled glutamate (black column) prevented L-[³H]glutamate uptake. NMO serum reduced L-[³H]glutamate uptake by 50%. The experiment shown in C was performed twice. All other experiments were done at least three times. The error bars represent the standard error of six and four replicates, respectively.

2474

SEQUELAE OF NMO-IGG-ASTROCYTIC AQP4 INTERACTIONS | Hinson et al.

in astrocytes would increase CNS microvascular endothelial permeability and promote inflammatory cell infiltration. Assembly of the final membrane attack complex might focally damage endfeet, where AQP4 is expressed most highly (6). However, a rich endowment of astrocytic membranes with complement regulatory proteins (10) may explain their relative resistance to AQP4-IgG–dependent lysis in this study, in comparison to AQP4-transfected human embryonic kidney (HEK)–293 cells (6).

## NMO–IgG attenuates Na+-dependent glutamate uptake in astrocytes

Glutamate toxicity is commonly postulated as a downstream mechanism mediating progression of neurodegenerative processes (for review see [11]). The CNS extracellular concentration of glutamate is elevated in many neurodegenerative diseases. Its excitotoxic effects on neurons are widely recognized. However, oligodendrocytes are highly sensitive to excitotoxic signals mediated by calcium-permeable glutamate receptors (AMPA and kainate types; for review see [12]) (13-15). It is plausible that glutamate toxicity may contribute to demyelination through an effect on oligodendroglia. These cells make and maintain the myelin sheaths that insulate CNS axons and are centrally involved in CNS inflammatory demyelinating disorders. A report that EAAT2 expression (Western blot and RT-PCR) is reduced in AQP4-null astrocytes (8) prompted us to evaluate glutamate toxicity as a potential outcome of IgG-induced AQP4 modulation. We hypothesized

that compromise of EAAT2 function through IgG-induced loss of AQP4 in NMO lesions might increase the extracellular concentration of glutamate in AQP4-rich regions critical to oligodendroglial and neuronal viability at nodes of Ranvier and perisynaptic regions (6).

First, we compared Na+-dependent glutamate transport in astrocytes exposed to NMO or control sera (Fig. 1 C). Uptake of L-[3H]glutamate was minimal (<200 counts/minute) in the absence of Na+ or when excess unlabeled glutamate was present. In the presence of Na+, L-[3H]glutamate uptake was increased to approximately 3,000 counts/min in cells unexposed to serum or exposed to control patient serum (Fig. 1 C). These results are consistent with the uptake of L-[3H]glutamate being Na+ dependent and glutamate specific. When serum containing NMO-IgG was added in these experimental conditions, L-[3H]glutamate uptake was reduced by ~50% (P < 0.0003; Fig. 1 C).

NMO–IgG down–regulates both EAAT2 and AQP4 from the surface of differentiated type 2 astrocytic cells

Attenuation of astrocytic L-[3H]glutamate uptake after exposure to NMO-IgG parallels the loss of AQP4 protein. To investigate the possibility that EAAT2 protein may be lost secondary to loss of surface AQP4, we used EAAT2-specific IgG to follow the fate of EAAT2 after exposing astrocytes to NMO-IgG. As noted by Stanimirovic et al. (16), we confirmed that EAAT1 and EAAT2 glutamate transporter levels in primary rat astrocyte membranes are too low to detect
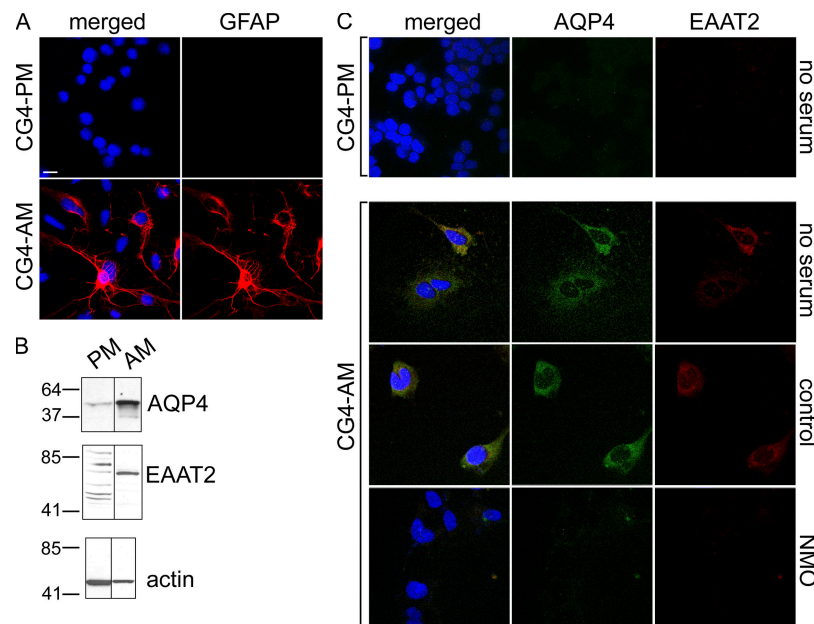
Figure 2. CG–4 glial cells in astrocytic differentiation medium up–regulate both AQP4 and EAAT2 expression; NMO serum down–regulates both. (A) CG-4 cells cultured in proliferation medium (CG4-PM) do not express cytoplasmic GFAP (red). After 7 d in astrocytic differentiation medium (CG4-AM), a subset of cells contains brilliant cytoplasmic GFAP. (B) The Western blot shows that undifferentiated CG4-PM (PM) cell lysates contain minimal EAAT2 or AQP4; both proteins are up-regulated in CG4-AM (AM). Markers indicate kilodalton reference standards. (C) AQP4 (green) and EAAT2 (red) are negligible in CG4-PM cells, but are up-regulated on the surface of CG4-AM cells; NMO serum, but not control patient serum, depletes both. DNA is blue (A and C). All experiments were performed a minimum of two times. Bars, 5 μm.

by immunofluorescence staining. We therefore investigated EAAT2 expression in the bipotential glial cell line CG-4, which is derived from O2-A progenitor cells in the developing rat CNS. In prescribed culture conditions (17), CG-4 cells differentiate into type 2 astrocytes. In proliferation-promoting medium (containing bFGF and PDGF), the cells (CG4-PM) lack GFAP intermediate filaments (Fig. 2 A). However, in medium with growth factors replaced by a high concentration of fetal bovine serum, type 2 astrocyte differentiation is evident in the cells (CG4-AM) by morphology and GFAP immunoreactivity (Fig. 2 A). In cells grown for 7 d in astrocyte differentiation medium, plasma membrane expression of both AQP4 and EAAT2 is enhanced (Fig. 2, B and C). However, when NMO serum is added to CG4-AM cells at day 7, both AQP4 and EAAT2 are depleted from the plasma membrane (Fig. 2 C). Addition of control sera in identical conditions does not discernibly affect expression of either AQP4 or EAAT2 (Fig. 2 C). Concomitant loss of both EAAT2 and AQP4 plausibly explains the reduced glutamate transport that we observed in cultured astrocytes exposed to NMO-IgG.

EAAT2 expression is up-regulated when AQP4 protein expression is induced in nonneural cells

AQP4 and EAAT2 are both enriched in the astrocytic endfoot membrane (18). Our finding that both are depleted from plasma membranes of cultured astrocytes exposed to NMO-IgG is consistent with the notion that EAAT2 expression depends on AQP4 expression. To further evaluate the relationship between AQP4 and glutamate transport, we studied the HEK-293 nonneural cell line, comparing EAAT2 expression in cells stably expressing GFP, GFP-AQP4, or a nonneural AQP, AQP5-GFP (Fig. 3). We readily detected EAAT1 in the plasma membranes of cell lines transfected with either GFP vector or GFP-AQP4 (Fig. 3 A). We did not detect EAAT2 in GFP vector-transfected cells (Fig. 3 B), but EAAT2 was strikingly upregulated in the plasma membrane of cells transgenically expressing either AQP4 or AQP5 (Fig. 3 B).

To determine whether this observed increase in membrane EAAT2 and functional glutamate transport might reflect an increase in EAAT2 gene transcription or protein expression, we examined EAAT2 transcripts by RT-PCR. The three transfected HEK-293 lines expressed EAAT2 transcripts at similar levels (Fig. 3 C). Western blot analyses (Fig. 3 D) supported our immunofluorescence observations that transgenic EAAT2 protein expression is upregulated when AQP4 or AQP5 is expressed in HEK-293 cells by comparison with cells transfected with vector alone. Expression of EAAT2 protein on the surface of cells expressing AQP might be increased through upregulated mRNA translation or, alternatively, through a posttranslational modification increasing EAAT2 protein stability or trafficking to the plasma membrane. These complementary observations accord with reports that EAAT2 protein expression is restricted to astrocytes, despite ubiquitous expression of EAAT2 mRNA (11). We conclude that restriction of EAAT2 expression to the

plasma membrane of astrocytes is determined by dependence on astrocytic AQP expression.

We confirmed that upregulated EAAT2 protein in GFP-AQP4 transfected cells was functional by demonstrating that GFP-AQP4 cells imported two- to threefold more glutamate via the Na^+-dependent pathway relative to GFP vector cells (P < 0.0002; Fig. 3 F). It is noteworthy that glutamate transport in Na^+-containing buffer was unchanged in GFP vector cells compared to GFP-AQP4 (Fig. 3 F). We anticipated that constitutively expressed EAAT1 in both cell lines would confer higher glutamate transport in GFP vector cells in Na^+-containing buffer than in buffer lacking Na^+. However, uptake of glutamate was unaffected in the presence of Na^+, suggesting that EAAT1 expressed constitutively in these cells is not functional.

Plasma membrane loss of EAAT2 after exposure to NMO serum is EAAT2-selective and is dependent on the presence of both AQP4 protein and NMO-IgG

Our data indicate that the concentration of AQP4 protein in the plasma membrane and Na^+-dependent glutamate transport are both reduced by exposure of primary astrocytes to NMO-IgG (Fig. 1). Our observations in differentiated CG-4 type 2 astrocytes suggest that the effect on glutamate transport in primary astrocytes is caused by plasma membrane loss of EAAT2 (Fig. 2). To further investigate the association between AQP4 and EAAT2, we evaluated the effect of NMO and control sera on both EAAT1 and EAAT2. Control serum did not appreciably affect localization or expression of the EAAT2 transporter. However, serum containing NMO-IgG induced rapid surface down-regulation of both GFP-AQP4 and EAAT2 (Fig. 4 A). Higher magnification (Fig. 4 A) revealed apparent colocalization of EAAT2 and AQP4 in early endosomal vesicles to which we previously demonstrated AQP4 translocation after exposure to NMO serum (6). We evaluated the localization of AQP4 and the early endosome antigen-1 marker after exposing the cells to NMO serum for 10 min. The white color that resulted when the images were merged suggested partial colocalization of AQP4 and EAAT2 in early endosomes (Fig. 4 B). However, separate vesicles in close proximity or overlapping in the z axis would yield the same result.

We excluded the possibility that NMO serum might contain EAAT2-specific IgG in addition to AQP4 IgG, by testing the effect of NMO serum on plasma membrane expression of EAAT2 in HEK-293 cells transfected with AQP5-GFP (Fig. 4 C). Those cells express both EAAT1 and EAAT2, but are devoid of AQP4 (Fig. 3). Exposure to NMO-IgG did not affect the distribution of EAAT1 or EAAT2 in AQP5-GFP cells (Fig. 4, C and E).

To investigate the specificity of EAAT2 down-regulation, we evaluated the effect of NMO-IgG on the EAAT1 glutamate transporter, which is expressed constitutively in nonneural HEK-293 cells (Fig. 3 E). NMO patient sera did not appreciably affect EAAT1 expression in these cells (Fig. 4 D),

in contrast to EAAT2 loss from the plasma membrane. These results imply a specific association between AQP4 and EAAT2 that does not exist for EAAT1. The rapid down-regulation of EAAT2 and AQP4 induced by NMO-IgG in GFP-AQP4-expressing cells and colocalization of both proteins in cytoplasmic endocytotic vesicles within 10 min is consistent with a direct effect of IgG on a surface macromolecular complex. The reduction in astrocytic glu-

tamate transport accompanying AQP4 down-regulation after exposure to NMO-IgG further supports our suggestion that AQP4 and EAAT2 are associated functionally in the plasma membrane.

AQP4 and EAAT2 coimmunoprecipitate

EAAT2 and EAAT1 are enriched in separate microdomains of the astrocytic plasma membrane (18, 19); EAAT2 is enriched
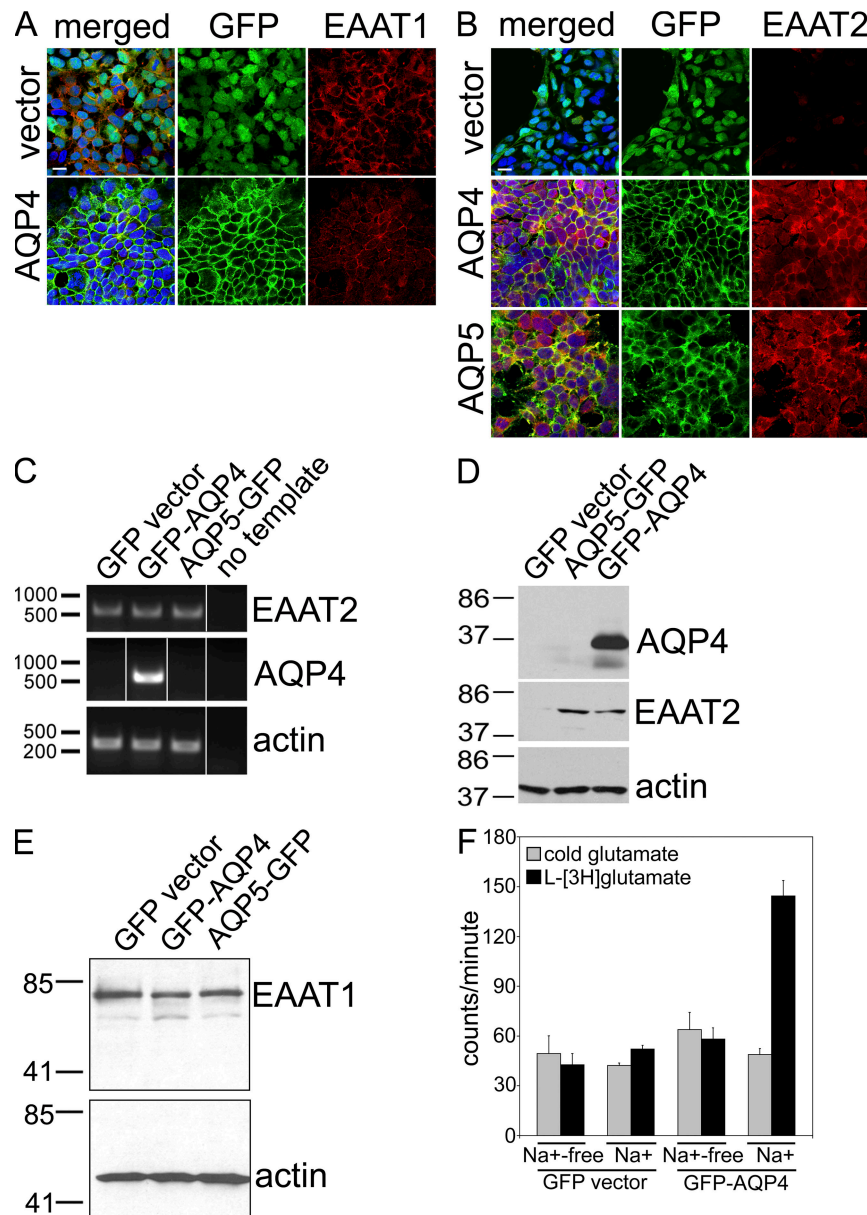

Figure 3. **Expression of AQP proteins in HEK-293 cells induces EAAT2 protein expression.** DNA is stained blue (A and B). (A) EAAT1 (red) is expressed constitutively, regardless of transfection. (B) EAAT2 (red) is localized in the plasma membrane of cells expressing AQP4 or AQP5 (green), but is undetectable in cells transfected with GFP-vector lacking an AQP cDNA. Bars, 10 μm. (C) For RT-PCR, all three cell lines express EAAT2 mRNA, regardless of AQP expression. Markers indicate basepair reference standards. (D) The Western blot shows that EAAT2 protein is up-regulated in cells transfected with AQP4 or AQP5, but not in GFP-vector–transfected cells. (E) EAAT1 protein and actin are expressed constitutively. Markers indicate kilodalton reference standards (D and E). (F) In glutamate transport experiments, GFP-AQP4 cells take up approximately threefold more L-[3H]glutamate than vector-transfected cells (note: Na+ dependence). All experiments were performed a minimum of two times. The error bars represent the standard error of six and four replicates, respectively.

in regions that highly express AQP4 (18). Our data suggest that EAAT2 and AQP4 exist as a macromolecular complex. When exposed to NMO-IgG, both are translocated from the plasma membrane to an endolysosomal-targeted population of cytoplasmic vesicles (Fig. 4, A and B). To evaluate potential physical interaction, we solubilized GFP-AQP4–transfected cells and probed the lysates with EAAT2-IgG. Addition of protein G–agarose captured both EAAT2 and AQP4 (Fig. 4 F). We obtained similar data using independent IgGs recognizing different EAAT2 epitopes (unpublished data). As a specificity control, we compared results obtained using EAAT1-IgG as a probe for the cell lysates. In contrast to EAAT2-IgG, EAAT1-IgG did not pull down AQP4. These results support the existence of AQP4 and EAAT2 as a macromolecular complex independent of EAAT1.

Colocalization of AQP4 and EAAT2 in CNS tissue

Our observations in primary astrocytes, type 2 differentiated CG-4 cells, and transfected nonneural HEK-293 cells indicate that the interaction of NMO-IgG with AQP4 induces at least three possible outcomes, each potentially pathogenic: (a) complement activation, (b) down-regulation of AQP4, and (c) coupled down-regulation of the EAAT2 glutamate transporter. Our immunohistochemical analysis of nonpathologic human CNS tissue (both cortical and spinal cord) reveal that EAAT2, but not EAAT1, normally colocalizes with AQP4 in gray matter astrocytes (Fig. 5 A) and that EAAT2 is most enriched in spinal cord gray matter (Fig. 5 B, top). These findings were reproducible and consistent with published rodent cord findings (19, 29).
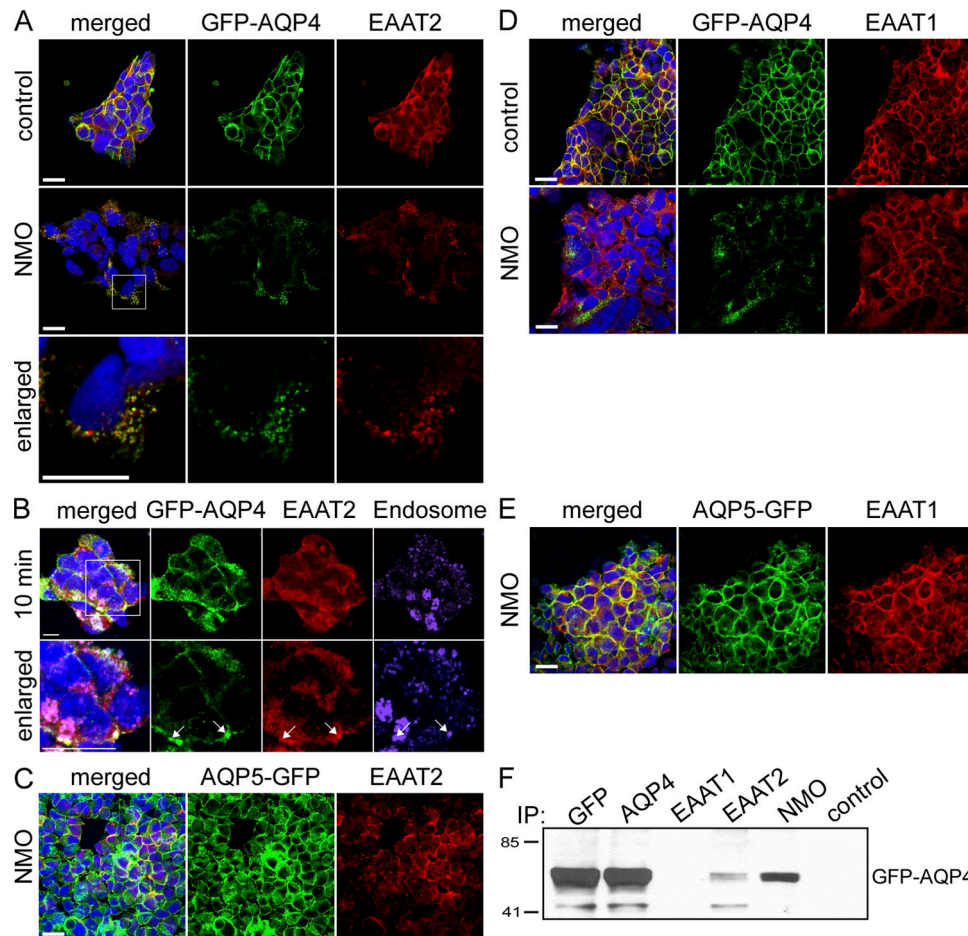
Figure 4. NMO-IgG modulation of AQP4 from transfected HEK-293 membranes down-regulates EAAT2 expression. GFP-AQP4– or AQP5-GFP–transfected cells (green) were probed with anti-EAAT2 or –EAAT1-IgG (red) after exposure to control or NMO patient serum (37°C; 4 h). Nuclear DNA is blue. (A) NMO serum caused membrane loss of both AQP4 and EAAT2; control serum did not affect the distribution of either. Enlarged images show both EAAT2 and AQP4 internalized in cytoplasmic vesicles after exposure to NMO serum. (B) Staining with early endosome marker (EEA1, purple) after 10-min exposure to NMO serum shows colocalization of both GFP-AQP4 and EAAT2 (arrows) in endocytotic vesicles (white spots in merged image). (A and B) Boxed areas are enlarged in the bottom image. (C) NMO serum does not selectively affect EAAT2 in cells transfected with AQP5. EAAT1 is not affected by NMO or control serum in cells transfected with AQP4 (D) or AQP5 (E). (F) Western blot shows NMO-IgG or IgG specific for GFP, AQP4, or EAAT2, capture GFP-AQP4 protein; GFP-AQP4 does not coprecipitate with control patient IgG or EAAT1-specific IgG. Markers indicate kilodalton reference standards. All experiments were performed a minimum of two times. Bars: (A, C, D, and E) 10 µm; or (B) 20 µm.

## NMO spinal cord lesions lack both AQP4 and EAAT2

Loss of AQP4 is a distinctive finding in both early and late lesions of NMO (4). NMO spinal cord tissue of normal appearance expresses normal levels of APQ4 and EAAT2 and lacks evidence of complement deposition (Fig. 5 B). Lesioned NMO spinal cord gray matter contrasts to normal appearing gray matter by exhibiting markedly reduced EAAT2, in addition to AQP4 loss and deposition of complement activation products (Fig. 5 B). Together, these findings are consistent with absence of EAAT2 staining being a biological phenomenon within the NMO lesion. AQP4 loss at sites of C9neo deposition is a representative finding in our nine previously published cases (4). EAAT2 loss may partially account for the destructive involvement of spinal cord gray matter which is characteristic of NMO. Lesions in MS CNS tissues are typically not necrotic. The marked loss of EAAT2 described in this report parallels loss of AQP4 in lesioned

NMO spinal cord tissue and contrasts with the increases in EAAT2 and AQP4 reported in both active and chronic MS lesions (20). We conclude that differences in regulation of glutamate homeostasis further distinguish NMO from classical MS (1).

Concluding remarks

The data we present from studies of living astrocytes, patient and control sera, normal human spinal cord tissue, and spinal cord tissues from a patient with typical NMO, both non-lesioned and lesioned, provide the first evidence supporting a pathogenic role for NMO-IgG in disrupting glutamate transport. Because astrocytes are relatively tolerant of increased glutamate concentrations (21), disruption of glutamate homeostasis by NMO-IgG has particular excitotoxic potential for neurons and oligodendrocytes. A focal increase of extracellular glutamate levels secondary to NMO-IgG–induced down-regulation of AQP4 may suffice to injure or kill oligodendrocytes that express calcium-permeable glutamate receptors (15, 22). Oligodendrocytes in the spinal cord and optic nerve, which are principal sites of demyelination in NMO, are particularly sensitive to changes in glutamate concentration. Modest elevation of extracellular glutamate concentration renders oligodendrocytes additionally susceptible to Ig-independent (alternative pathway) complement attack (23). The potential pathogenic sequelae we demonstrate in this study for NMO-IgG binding to AQP4-rich membranes in primary astrocytes are both competing and cooperative. Depletion of AQP4 water channels in the plasma membrane would disrupt water homeostasis and promote edema. If complement were lacking, the consequences of impaired glutamate transport would be particularly deleterious for oligodendrocytes and neurons.

Outcomes of therapies directed at glutamate receptors have been unimpressive for neurodegenerative conditions where glutamate toxicity has been implicated in disease progression (for review see [24]). However, our demonstration that the major astrocytic glutamate transporter EAAT2 exists in a macromolecular complex with the AQP4 water channel, and is down-regulated by AQP4-specific autoantibodies that are restricted to patients with the NMO-spectrum of CNS inflammatory autoimmune demyelinating disorders, has unanticipated pathogenic implications for glutamate toxicity as a central mechanism in a spectrum of disorders that are commonly mistaken for MS. NMO is now recognized as a potentially reversible IgG-mediated attack on astrocytic water channels (1). The results we obtained from studies of serum and spinal cord tissue of patients with NMO hold promise for novel therapeutic strategies for the management of NMO-spectrum disorders. For example, it might be feasible to ameliorate tissue damage in both gray and white matter if therapeutic upregulation of EAAT2 can be achieved in patients whose neurological dysfunction is attributable to AQP4 autoimmunity.
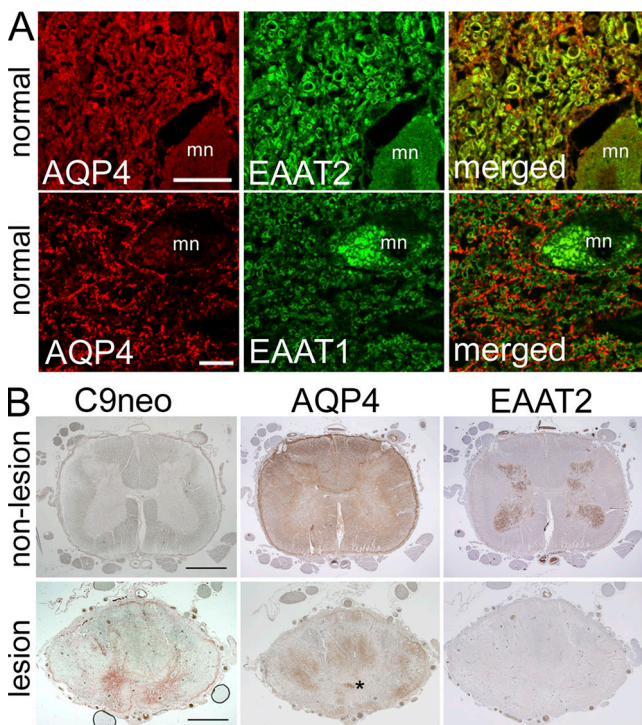
Figure 5. Glutamate transporter expression in human tissue.
(A) Normal spinal cord from a single subject. Duplicate sections were dual stained for AQP4 (red) and EAAT2 or EAAT1 (green), i.e., four sections. Merged images show AQP4 and EAAT2 colocalization (top, yellow), but no colocalization of AQP4 and EAAT1 (bottom); mn, motor neuron. (B) Spinal cord tissue from a single NMO-IgG–seropositive patient. Three sections of nonlesioned lumbar region (top) serve as staining control for lesioned cord (bottom). The lack of complement deposition (C9neo, brick red in lesioned cord, bottom) and high expression of AQP4 in both white and gray matter are typical of normal cord tissue; EAAT2 is highly enriched in gray matter. Prominent deposition of C9neo in gray matter of lesioned thoracic cord (bottom, same patient) corresponds to focal regions of AQP4 and EAAT2 loss in adjacent sections. AQP4 is partially retained in the white matter. Asterisk, central canal. Bars: (A) 20 μm; (B) 200 μm.

MATERIALS AND METHODS

Cell lines and transgenic constructs. Primary astrocytes isolated from cerebral cortices of P1-3 rats (provided by D. Edberg, Mayo Clinic, Rochester, MN) and the rat brain–derived O-2A progenitor cell line CG-4 were grown as previously described (17, 25). We previously described the GFP-AQP4 construct and stably transfected HEK cell lines (HEK-293) (2, 6). We amplified AQP5 from a human salivary gland cDNA library, inserted it into pEGFP-N1 vector (Clontech Laboratories), and transfected (Fugene 6) HEK-293 cells with the parent vector or vector containing AQP5 transgenes. Stable clones were maintained in DMEM supplemented with 10% bovine calf serum and antibiotics.

Antibodies and human sera. We purchased fluorochrome-conjugated goat IgGs from Invitrogen (Alexa Fluor 546; human, mouse, or rabbit IgG-specific, and Oregon Green; mouse IgG-specific; Cy5; rabbit IgG-specific) and goat IgGs monospecific for human IgG (TRITC-conjugated) or human IgM (FITC-conjugated) from SouthernBiotech. Rabbit IgG specific for AQP4 (residues 249–323) was purchased from Sigma-Aldrich, rabbit IgG specific for EAAT1 was obtained from Santa Cruz, and rabbit IgG specific for EAAT2 was purchased from either Santa Cruz Biotechnologies (Western blotting and immunoprecipitation) or AbCam (immunofluorescence). We purchased mouse monoclonal IgGs from AbCam (anti-EEA1), Sigma-Aldrich (anti-GFAP conjugated to Cy3), BD Biosciences (anti-EAAT2), and Santa Cruz Biotechnologies (anti-GFP). De-identified sera from NMO and control patients were obtained, with Mayo Clinic IRB approval, from the Neuroimmunology Laboratory, Department of Laboratory Medicine and Pathology, Mayo Clinic Rochester, MN (6).

Immunostaining. Cell lines grown on glass coverslips were rinsed in PBS and fixed in 4% PFA, for 20 min at room temperature. After holding 30 min in 9% normal goat serum/0.1% Triton X-100, they were held at 4°C overnight in defined antibodies diluted in 10% normal goat serum, washed in PBS, and held for 60 min at room temperature in appropriate secondary antibody diluted in 10% normal goat serum. After washing in PBS and mounting on a slide with ProLong Gold DAPI antifade medium (Invitrogen), fluorochrome-labeled cells were imaged using a confocal microscope (model LSM510; Carl Zeiss, Inc.).

Sections of archival CNS tissues derived from control and NMO patients (5 μm; formalin-fixed and paraffin-embedded) were stained with hematoxylin and eosin (HE), Luxol-fast blue-periodic acid-Schiff (LFB/PAS), or Bielschowsky silver impregnation. We performed avidin-biotin–based immunohistochemistry without modification (26), by incubating tissue sections for 1 h with 10% normal goat serum, and holding overnight at 4°C with and without primary antibodies.

Antigen modulation assay. We dispensed cells onto glass coverslips coated with laminin (CG-4) or poly-L-lysine (HEK-293 and primary rat astrocytes; BioCoat; BD Biosciences). After at least 48 h, we added control or NMO serum at 20% final concentration (with complement inactivated by holding 30 min at 56°C) and processed the cells for immunofluorescence analysis.

Complement membrane lesioning. Growth medium of confluent primary astrocytes growing in 6-well plates was replaced with fresh medium containing 20% NMO or control sera. After 15 min at room temperature, we added fresh or heat–inactivated complement (Low–Tox-H rabbit complement; Cedarlane Laboratories; final concentration 20%), held them 40 min at 37°C, and then processed them for flow cytometric analysis (6).

Glutamate uptake assay. We measured Na^+–dependent radiolabeled glutamate uptake (27) using primary astrocytes grown to confluence in 24-well dishes. After rinsing with 50 mM Tris-HCl and 320 mM sucrose, pH 7.4, we incubated control wells for 15 min with 10 mM unlabeled L-glutamate, then added L-[^{3}H]glutamate (0.1 μCi; GE Healthcare; specific activity = 55.0 μCi/nmol) in 25 mM NaHCO$_3$, 5 mM KCl, 1 mM KH$_2$PO$_4$, 1 mM MgSO$_4$, 2 mM CaCl$_2$, and 555 mM D-glucose, pH 7.4, with or without

Na^+ (Krebs buffer containing 120 mM NaCl, or 120 mM choline chloride, in 25 mM Tris, 5 mM KCl, 1 mM KH$_2$PO$_4$, 1 mM MgSO$_4$, 2 mM CaCl$_2$, and 555 mM D-glucose, pH 7.4). Both buffers contained 40 μM unlabeled glutamate. After 5 min at 37°C, we transferred the cells to 4°C, washed extensively with PBS, lysed in 0.1 M NaOH, and measured uptake of radiolabeled glutamate using a Beckman Coulter LS 6000SC scintillation counter. For all experimental conditions, we performed quadruplicate assays and calculated glutamate uptake as counts/minute/well, with and without Na^+.

To assay glutamate uptake in GFP vector and GFP-AQP4 stable HEK-293 cells, we used an alternative HEK-293–optimized protocol (28). We defined EAAT2-specific transport as the difference in glutamate uptake between GFP vector cells and GFP-AQP4–transfected cells.

Isolation of RNA and RT–PCR analysis. We isolated total RNA from trizol-lysed cells, and generated double-stranded cDNA using Superscript III First Strand Synthesis kit with random hexamer primers (according to Invitrogen protocols). To avoid amplifying contaminating genomic DNA, we used primer pairs that anneal in adjacent exons, as follows: AQP4 (forward, 5′-TGCACCAGGAA-GATCAGCATCG-3′; reverse, 5′-CAGGTCATCCGTCTCTACCTG-3′) and EAAT2 (forward, 5′-GGTGGAAGTGCGAATGCACGACAGTCATC-3′; reverse, 5′-CCTCGTCTGGCGGTGGTGCAACCAGGAC-3′). We amplified β-actin as a control.

Immunoprecipitation and Western blot. Protocols were as previously described (2). Commercial antibodies (AQP4, EAAT1, EAAT2, or GFP; 2 μg/ml), or human sera (a high-titer pool of NMO patient or control patient sera; 30 μl/ml) were used as probes. Immune complexes released from protein G-agarose were resolved by electrophoresis (4–15% gradient polyacrylamide, room temperature). We exposed transblotted, blocked proteins for 1 h to IgG specific for the following: GFP (1:1,000), AQP4 (1:500), EAAT1 (1:200), actin (1:2,000), or EAAT2 (1:200); we then probed the proteins with horseradish peroxidase–conjugated goat anti–mouse IgG or goat anti–rabbit IgG, and detected bound IgG autoradiographically (SuperSignal West Pico Chemiluminescence; Thermo Fisher Scientific).

Statistical analysis. We calculated significance using the Student's *t* test (two-tailed).

REFERENCES

1. Wingerchuk, D.M., V.A. Lennon, C.F. Lucchinetti, S.J. Pittock, and B.G. Weinshenker. 2007. The spectrum of neuromyelitis optica. *Lancet Neurol.* 6:805–815.
2. Lennon, V.A., T.J. Kryzer, S.J. Pittock, A.S. Verkman, and S.R. Hinson. 2005. IgG marker of optic-spinal multiple sclerosis binds to the aquaporin-4 water channel. *J. Exp. Med.* 202:473–477.
3. Nakamura, M., I. Miyazawa, K. Fujihara, I. Nakashima, T. Misu, S. Watanabe, T. Takahashi, and Y. Itoyama. 2008. Preferential spinal central gray matter involvement in neuromyelitis optica. An MRI study. *J. Neurol.* 255:163–170.
4. Roemer, S.F., J.E. Parisi, V.A. Lennon, E.E. Benarroch, H. Lassmann, W. Bruck, R.N. Mandler, B.G. Weinshenker, S.J. Pittock, D.M.

Wingerchuk, and C.F. Lucchinetti. 2007. Pattern-specific loss of aquaporin-4 immunoreactivity distinguishes neuromyelitis optica from multiple sclerosis. *Brain*. 130:1194–1205.

5. Lucchinetti, C.F., R.N. Mandler, D. McGavern, W. Bruck, G. Gleich, R.M. Ransohoff, C. Trebst, B.G. Weinshenker, D. Wingerchuk, J.E. Parisi, and H. Lassmann. 2002. A role for humoral mechanisms in the pathogenesis of Devic's neuromyelitis optica. *Brain*. 125:1450–1461.

6. Hinson, S.R., S.J. Pittock, C.F. Lucchinetti, S.F. Roemer, J.P. Fryer, T.J. Kryzer, and V.A. Lennon. 2007. Pathogenic potential of IgG binding to water channel extracellular domain in neuromyelitis optica. *Neurology*. 69:2221–2231.

7. Pittock, S.J., V.A. Lennon, J. de Seze, P. Vermersch, H.A. Homburger, D.M. Wingerchuck, C.F. Lucchinetti, H. Zephir, K. Moder, and B.G. Weinshenker. 2008. Neuromyelitis optica and non organ-specific autoimmunity. *Arch. Neurol*. 65:78–83.

8. Zeng, X.N., X.L. Sun, L. Gao, Y. Fan, J.H. Ding, and G. Hu. 2007. Aquaporin-4 deficiency down-regulates glutamate uptake and GLT-1 expression in astrocytes. *Mol. Cell. Neurosci*. 34:34–39.

9. Danbolt, N.C., J. Storm-Mathisen, and B.I. Kanner. 1992. An [Na+ + K+]coupled L-glutamate transporter purified from rat brain is located in glial cell processes. *Neuroscience*. 51:295–310.

10. Morgan, B.P., and P. Gasque. 1996. Expression of complement in the brain: role in health and disease. *Immunol. Today*. 17:461–466.

11. Danbolt, N.C. 2001. Glutamate uptake. *Prog. Neurobiol*. 65:1–105.

12. Matute, C., E. Alberdi, M. Domercq, F. Pérez-Cerdá, A. Pérez-Samartin, and M.V. Sánchez-Gómez. 2001. The link between excitotoxic oligodendroglial death and demyelinating diseases. *Trends Neurosci*. 24:224–230.

13. Matute, C., M. Domercq, D.J. Fogarty, M. Pascual de Zulueta, and M.V. Sánchez-Gómez. 1999. On how altered glutamate homeostasis may contribute to demyelinating diseases of the CNS. *Adv. Exp. Med. Biol*. 468:97–107.

14. Smith, T., A. Groom, B. Zhu, and L. Turski. 2000. Autoimmune encephalomyelitis ameliorated by AMPA antagonists. *Nat. Med*. 6:62–66.

15. Pitt, D., P. Werner, and C.S. Raine. 2000. Glutamate excitotoxicity in a model of multiple sclerosis. *Nat. Med*. 6:67–70.

16. Stanimirovic, D.B., R. Ball, D.L. Small, and A. Muruganandam. 1999. Developmental regulation of glutamate transporters and glutamine synthetase activity in astrocyte cultures differentiated in vitro. *Int. J. Dev. Neurosci*. 17:173–184.

17. Louis, J.C., E. Magal, D. Muir, M. Manthorpe, and S. Varon. 1992. CG-4, a new bipotential glial cell line from rat brain, is capable of differentiating in vitro into either mature oligodendrocytes or type-2 astrocytes. *J. Neurosci. Res*. 31:193–204.

18. Nielsen, S., E.A. Nagelhus, M. Amiry-Moghaddam, C. Bourque, P. Agre, and O.P. Ottersen. 1997. Specialized membrane domains for water transport in glial cells: high-resolution immunogold cytochemistry of aquaporin-4 in rat brain. *J. Neurosci*. 17:171–180.

19. Chaudhry, F.A., K.P. Lehre, M. van Lookeren Campagne, O.P. Ottersen, N.C. Danbolt, and J. Storm-Mathisen. 1995. Glutamate transporters in glial plasma membranes: highly differentiated localizations revealed by quantitative ultrastructural immunocytochemistry. *Neuron*. 15:711–720.

20. Newcombe, J., A. Uddin, R. Dove, B. Patel, L. Turski, Y. Nishizawa, and T. Smith. 2008. Glutamate receptor expression in multiple sclerosis lesions. *Brain Pathol*. 18:52–61.

21. McDonald, J.W., S.P. Althomsons, K.L. Hyrc, D.W. Choi, and M.P. Goldberg. 1998. Oligodendrocytes from forebrain are highly vulnerable to AMPA/kainite receptor-mediated excitotoxicity. *Nat. Med*. 4:291–297.

22. Salter, M.G., and R. Fern. 2005. NMDA receptors are expressed in developing oligodendrocyte processes and mediate injury. *Nature*. 438:1167–1171.

23. Alberdi, E., M.V. Sánchez-Gómez, I. Torre, M. Domercq, A. Pérez-Samartin, F. Pérez-Cerdá, and C. Matute. 2006. Activation of kainate receptors sensitizes oligodendrocytes to complement attack. *J. Neurosci*. 26:3220–3228.

24. Kemp, J.A., and R.M. McKernan. 2002. NMDA receptor pathways as drug targets. *Nat. Neurosci*. 5:1039–1042.

25. Garlin, A.B., A.D. Sinor, J.D. Sinor, S.H. Jee, J.B. Grinspan, and M.B. Robinson. 1995. Pharmacology of sodium-dependent high-affinity L-[3H]glutamate transport in glial cultures. *J. Neurochem*. 64:2572–2580.

26. Vass, K., H. Lassmann, H. Wekerle, and H.M. Wisniewski. 1986. The distribution of Ia antigen in the lesions of rat acute experimental allergic encephalomyelitis. *Acta Neuropathologica (Berl.)*. 70:149–160.

27. Lin, C.I., I. Orlov, A.M. Ruggerio, M. Dykes-Hober, A. Lee, M. Jackson, and J.J.D. Rothstein. 2001. Modulation of the neuronal glutamate transporter EAAC1 by an interacting protein GTRAP3-18. *Nature*. 410:84–88.

28. Jensen, A.A., and H. Bräuner-Osborne. 2004. Pharmacological characterization of human excitatory amino acid transporters EAAT1, EAAT2 and EAAT3 in a fluorescence-based membrane potential assay. *Biochem. Pharmacol*. 67:2115–2127.

29. Queen, S.A., P. Kesslack, and R.J. Bridges. 2007. Regional distribution of sodium-dependent excitatory amino acid transporters in rat spinal cord. *J. Spinal Cord Med*. 30:263–271.